UNCLASSIFIED

NRL Report 6385

Optical Calibration Analysis of the U.S. Naval Space Surveillance System

L. O. Hayden and T. B. McCaskill

Space Surveillance Branch
Applications Research Division

April 25, 1966

U.S. NAVAL RESEARCH LABORATORY
Washington, D.C.

DISTRIBUTION OF THIS DOCUMENT IS UNLIMITED

UNCLASSIFIED

CONTENTS

Abstract	ii
Problem Status	ii
Authorization	ii
INTRODUCTION	1
GEOMETRIC CONSIDERATIONS IN THE SPACE SURVEILLANCE ANTENNA SYSTEM	1
DERIVED RELATIONSHIPS OF MULTIANTENNA SYSTEMS	3
GEOMETRY OF THE TRANSMISSION PATH	4
RECEIVING SYSTEM ANTENNAS	5
ELECTRONIC PHASE-MEASURING EQUIPMENT	9
SYSTEM OUTPUTS	10
REVIEW OF EARLIER OPTICAL CALIBRATION	10
NEW FORM OF DATA SUMMARY	12
SCATTER OF POINTS	15
MISCELLANEOUS TOPICS	20
CONCLUDING REMARKS	22
ACKNOWLEDGMENTS	22
REFERENCES	23

ABSTRACT

A preliminary optical calibration of the U.S. Naval Space Surveillance System was made in 1961 using graphical methods. Since then, calibration has been continued using better equipment and data reduction methods to determine more precisely the characteristics of the system. It is shown that the 108-MHz system studied is capable of measuring angles within a standard deviation σ of 1/2 min of arc at zenith.

Electronic calibration methods used in setting up the 108-MHz system are shown to have a mean accuracy of approximately 3.5 percent of a wavelength for baselines up through 520 ft in length. Bias errors for baselines of 1040 ft and longer are larger than for the shorter baselines and must be corrected to obtain maximum accuracy from the system.

Baselines in the range of 16 to 520 ft have (for Echo passes) a mean standard deviation of $\pm 0.034\lambda$, which is independent of baseline length and angle of arrival and is internal to the system. The random error for longer baselines increases until it reaches a mean standard deviation of $\pm 0.09\lambda$ for the 5200-ft baseline.

PROBLEM STATUS

This is a final report on the 108-MHz system; work on a 216-MHz system is continuing.

AUTHORIZATION

NRL Problem R02-35
Project RT 8801-001/6521/S434-00-01

Manuscript submitted January 10, 1966.

UNCLASSIFIED

OPTICAL CALIBRATION ANALYSIS OF THE U.S. NAVAL SPACE SURVEILLANCE SYSTEM

INTRODUCTION

The U.S. Naval Space Surveillance System (1) is a multistatic radar containing four radio-interferometer-type receiving stations and three transmitting stations located along a great circle which crosses the southern part of the United States. The transmitting and receiving antennas form fan-shaped patterns in the plane of the great circle through the stations. Hence the region of detection is a vertical wedge of small angular cross section which is bisected by the plane of the great circle (or "fence"). As a satellite crosses the fence, the phase measurements obtained from a set of antenna pairs spaced along the great circle* and a set perpendicular to it determine two direction angles from the receiving station to the satellite.

The phase measurements, from which the direction angles are obtained, would contain bias errors unless the surveillance system were calibrated. The first calibration was done by using the Vanguard I satellite, 1958 Beta 1, the orbit of which had been determined by the Minitrack system. The Minitrack system had been calibrated, in turn, with reference to the stars (2). With the launching of the Echo I satellite, direct calibration of the system became possible. In anticipation of the launching of the Echo I satellite, a project to calibrate the Space Surveillance system by direct optical means was undertaken in April 1960. A minimum accuracy of 0.1 degree was set as an initial goal. This goal was met in the preliminary calibration, which was completed in 1961. A simple graphical method of data reduction was used at that time (3). To refine further the calibration of the Space Surveillance system, optical calibration has been improved by the use of a comparator engine and by computer reduction of the data. An analysis of this work and a brief summary of earlier work are given in the present report.

GEOMETRIC CONSIDERATIONS IN THE SPACE SURVEILLANCE ANTENNA SYSTEM†

Let us consider a set of Cartesian coordinates (Fig. 1) with the coordinate axes x and y lying in the horizontal plane and parallel to the east-west and north-south baselines, respectively. Antenna arrays are centered at the points a, d, and f. The distances ad and af are called baselines.

If signals arrive at these antennas from a sufficiently great distance, the rays may be considered parallel.‡ The differences in distance from the satellite to a and d is aL, and to a and f is aM. The direction cosines to the satellite are given by

*These antenna pairs generate the so-called east-west and north-south baselines which differ by a few degrees, depending on the location along the fence, from the indicated geographical directions.

†The geometric arrangement of the Minitrack-type interferometer may be found in the literature. It is repeated here as a base for further mathematical treatment pertinent to this report. (See Ref. 4.)

‡The maximum hyperbolic error introduced in this approximation for a 100-mi-high satellite is about 1 sec of arc for a 5200-ft baseline.

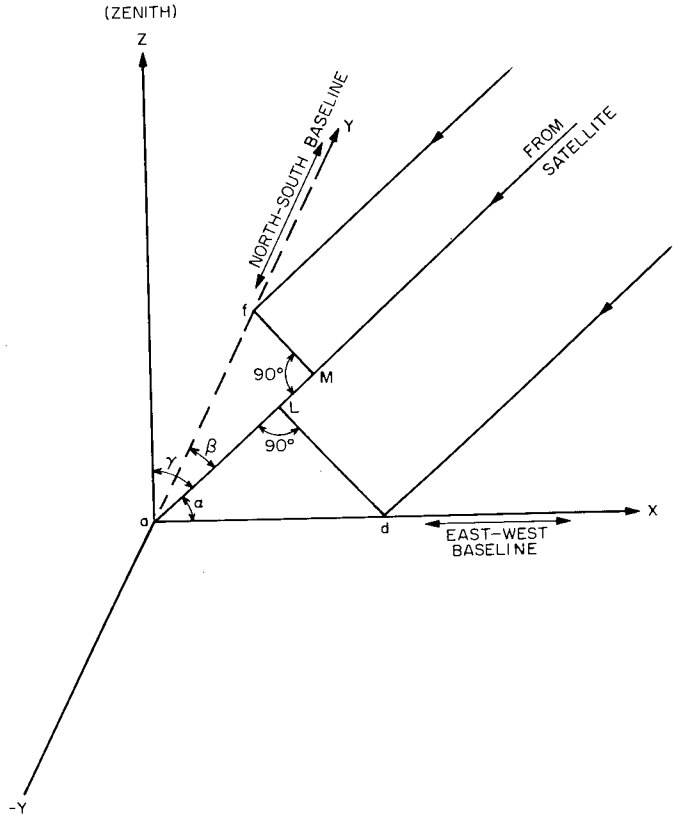

Fig. 1 - Coordinate system setup for the Space Surveillance system antennas. Antenna arrays are located at a, d, and f. The baseline af is oriented in a (approx.) north-south direction, and ad is in an (approx.) east-west direction. The direction of the incoming signals from a distant satellite is given by the direction angles α, β, and γ.

$$\cos \alpha = aL/ad \tag{1}$$

$$\cos \beta = aM/af . \tag{2}$$

Similar equations can be written for other antenna pairs with different spacings. Since the electronic equipment will measure phase differences between pairs of antenna, it is advantageous to express the distances in Eqs. (1) and (2) in terms of wavelength. Accordingly, one may write for the ith and jth baselines

$$\cos \alpha = \frac{n_i + \phi_i}{B_i} \tag{3}$$

and

$$\cos \beta = \frac{m_j + \omega_j}{B_j} \tag{4}$$

in which the right-hand terms are measured in wavelength. The subscript i indicates a value associated with a baseline B_i along the x axis; similarly, j indicates a value for a baseline B_j along the y axis. The quantities n_i and m_j have integral values (0, ±1, ±2, ±3, . . .)* and ϕ_i and ω_j are the remaining fractional parts of the difference in path length. Inasmuch as all signals must arrive from the hemisphere above the earth's horizon, the direction angle γ is restricted to the values from zero to $\pi/2$.

The antenna pattern of the U.S. Naval Space Surveillance System confines the response of the antennas to a small angular wedge in the neighborhood of the xz plane. It is convenient to choose the moment when $\beta = \pi/2$. This restriction leaves only one angle as a variable. With this restriction the zenith angle θ may be substituted for the direction angle α according to the relationship

$$\theta = (\pi/2) - \alpha.^{\dagger} \tag{5}$$

Using this relationship, Eq. (3) for the ith baseline is transformed to

$$\sin\theta = \frac{n_i + \phi_i}{B_i}. \tag{6}$$

This is the familiar form of the interferometer equation as used in space surveillance work. In Eq. (6) B_i is determined by a survey, and ϕ_i is measured by the electronic system. Since two unknowns (θ and n_i) remain, the equation cannot be solved without some further restrictions.

If $B < (\lambda/2) - \epsilon$, Eq. (6) will have a unique solution‡ since $n + \phi$ is then single valued for the allowable range of θ. For a frequency of 108 MHz, setting B_i equal to 4 ft satisfies the above condition. Alternatively, choosing a pair of baselines such that

$$B_{k+1} - B_k < (\lambda/2) - \epsilon \tag{7}$$

provides a unique solution§ to Eq. (6). The inequality, Eq. (7), allows wider separation of antenna arrays so that the same antennas which resolved the basic ambiguity can be used as two longer baselines of the system.

DERIVED RELATIONSHIPS OF MULTIANTENNA SYSTEMS

Taking the derivative of Eq. (6) with respect to θ, between jumps in n one obtains

$$\frac{d\phi_i}{d\theta} = B_i \cos\theta, \tag{8}$$

---

*$|n_i|$ and $|m_j|$ never exceed $B_i + 1$ or $B_j + 1$, respectively.

†θ is positive when $\alpha < \pi/2$ and negative when $\alpha > \pi/2$.

‡ϵ is a positive constant, the size of which depends on the maximum error in the measurement of phase. The $(\lambda/2) - \epsilon$ limit on separation of baselines assumes a 180-degree range in direction of signal arrival. If this range is restricted, an increase in the length of the shortest baseline is made possible. For instance, if the system responds to signals over a range $\delta\beta$ of $90 \pm 1/2$ degrees, one obtains, by substituting these values of β in the derivative of Eq. (4), the baseline length B as follows:

$$\delta(m + \omega) = 1\lambda = B\delta(\cos\beta) = B[\cos(90 - 1/2) - \cos(90 + 1/2)]$$

from which

$$B = \frac{1\lambda}{0.01746} \approx 500 \text{ ft (at 108 MHz)}.$$

Hence, with a beamwidth of 1 degree, the shortest north-south baseline can be as long as 500 ft.

§If $B_k \to 0$, the inequality, Eq. (7), degenerates to the inequality for a single short baseline.

which shows that the dependence of the phase ϕ on zenith angle is directly proportional to baseline length and the cosine of the zenith angle. Forming the ratio of two equations like Eq. (8) gives

$$\frac{\frac{d}{d\theta}(\phi_{k+1})}{\frac{d}{d\theta}(\phi_k)} = \frac{B_{k+1}}{B_k}, \tag{9}$$

which shows that the relative ability to measure the change in arrival angle depends on the ratio of baseline lengths and on no other geometric factors.

For a practical system, a very short baseline, or equivalent, satisfying the inequality, Eq. (7), is required to resolve an initial ambiguity in direction, and the longest possible antenna is indicated to obtain maximum sensitivity to angle change according to Eq. (8). Intermediate-size baselines will be required to assure correct resolution because of limited precision in the measurement of ϕ. By equating the solutions of zenith angle by Eq. (6) for two baselines, k and $k+1$, and solving for n_{k+1}, one obtains

$$n_{k+1} = \left(\frac{B_{k+1}}{B_k}\right) n_k + \left(\frac{B_{k+1}}{B_k}\right) \phi_k - \phi_{k+1}. \tag{10}$$

Let us assume that errors are insignificant, except in the measurement of phase. Then the unambiguous determination of n_{k+1} when n_k is already known is

$$|\delta n_{k+1}| = \left|\left(\frac{B_{k+1}}{B_k}\right) \delta\phi_k - \delta\phi_{k+1}\right| < 0.5. \tag{11}$$

It is clear from Eq. (11) that $\delta\phi_k$ is more significant than $\delta\phi_{k+1}$, by the ratio of baseline lengths, in determining the correct value of n_{k+1}. The inequality, Eq. (11), establishes conditions for correctly determining all n_i's except n_1. Further investigation of this relationship will be taken up when observational data is examined.

For some problems the phase and phase rate during the entire period of signal detection is of interest. The angle θ is not applicable for those problems. Time rates may be derived from Eqs. (3) and (4) by differentiating with respect to time, which yields

$$\frac{d\alpha}{dt} = -\frac{\phi_i}{B_i \sin \alpha} \tag{12}$$

and

$$\frac{d\beta}{dt} = -\frac{\dot{\omega}_j}{B_j \sin \beta}. \tag{13}$$

These relations may be compared with optically measured values of $\sin \alpha$, $d\alpha/dt$, $\sin \beta$, and $d\beta/dt$.

GEOMETRY OF THE TRANSMISSION PATH

The earlier Minitrack calibration method (2) used aircraft as calibration objects. The altitude of these objects was such as to require hyperbolic corrections. In the present study, the calibration signal source is the Echo I satellite. This object is high enough so that hyperbolic corrections are unnecessary. When a satellite S is used as the optical

source, Fig. 2(a), the light follows the path $SP'P$ from the satellite to the camera, undergoing appreciable bending in the last few miles of the atmosphere by an amount

$$\Delta\theta_{sex} = \theta - \theta_{sex} . \tag{14}$$

The error $\Delta\theta_{sex}$ in measurements made with a sextant or other gravity referenced instrument increases with zenith angle to 9.9 min of arc (5) for a zenith angle of 85 degrees, which is the largest zenith angle considered in this study. However, in our work the angle to the satellite is determined with respect to the background stars, which is equivalent to having the camera located at point P' and measuring the angle θ_o. The error $\Delta\theta$, in seconds of arc, resulting from treating θ_o as the true angle to the satellite is*

$$\Delta\theta = \theta_o - \theta = \frac{435.0 \tan \theta}{r \cos \theta} \left(1 - e^{-0.1385 r \cos \theta}\right) \tag{15}$$

in which r is the magnitude of the slant range in kilometers. This error is negligible in comparison with other limitations of the system.

The radio path to the satellite S is represented by two parallel rays, Fig. 2(b), entering the lower atmosphere at a zenith angle θ_r. The phase difference between the two points P_1' and P_2' is $n + \phi$. Since $P_1P_1' = P_2P_2'$, $n + \phi$ is the phase difference between the two antennas at P_1 and P_2. The effect is similar to having the receivers located at the top of the lower atmosphere where bending in the lower atmosphere begins. Hence, except for differences which may exist between the index of refraction of air for optical wavelengths and for 108 MHz, the error-correcting behavior is the same, and the error is quite small in each case because of the relative thinness of the lower atmosphere as compared with the height of the satellite.

RECEIVING SYSTEM ANTENNAS

Figure 3(a) gives the antenna layout which existed at the time of the measurements for the receiving station at Fort Stewart, Georgia. The arrays 1, 2, 3, 4, and 5 are each composed of four 400-ft sections A, B, C, and D. Arrays 6 and 7 have only one 400-ft section. The outputs from the four sections of arrays 1-5 are combined after separate preamplification to supply the signal for one element of a baseline pair. North-south baselines are formed from pairs of 400-ft sections to give north-south baselines of 400, 800, 1200, and 1852 ft. Note that baselines from 16 ft to 204 ft use 1600-ft sections, and all longer east-west pairs and north-south pairs use 400-ft sections. All antenna sections at the Ft. Stewart station use dipole elements above ground screens.

Figure 3(b) gives the antenna layout for the Silver Lake, Elephant Butte, and San Diego receiving stations. Each letter designates an antenna array 400-ft long. Pairs of these arrays form baseline lengths up to 5200 ft. Perpendicular to the east-west baselines, combinations a, f, j, and k provide capability of 400, 800, and 1200-ft north-south baselines. Sections p, r, n, and m are yagi antennas without ground screens; all other sections are composed of dipoles with ground screens. At San Diego only, 400-ft sections are located east of section f and north of sections c and d to form 4- and 8-ft baselines. These are shown on the drawings by dashed lines.

*The error $\Delta\theta$ using a high satellite is on the order of 1 sec of arc for low angles. (See Ref. 6.)

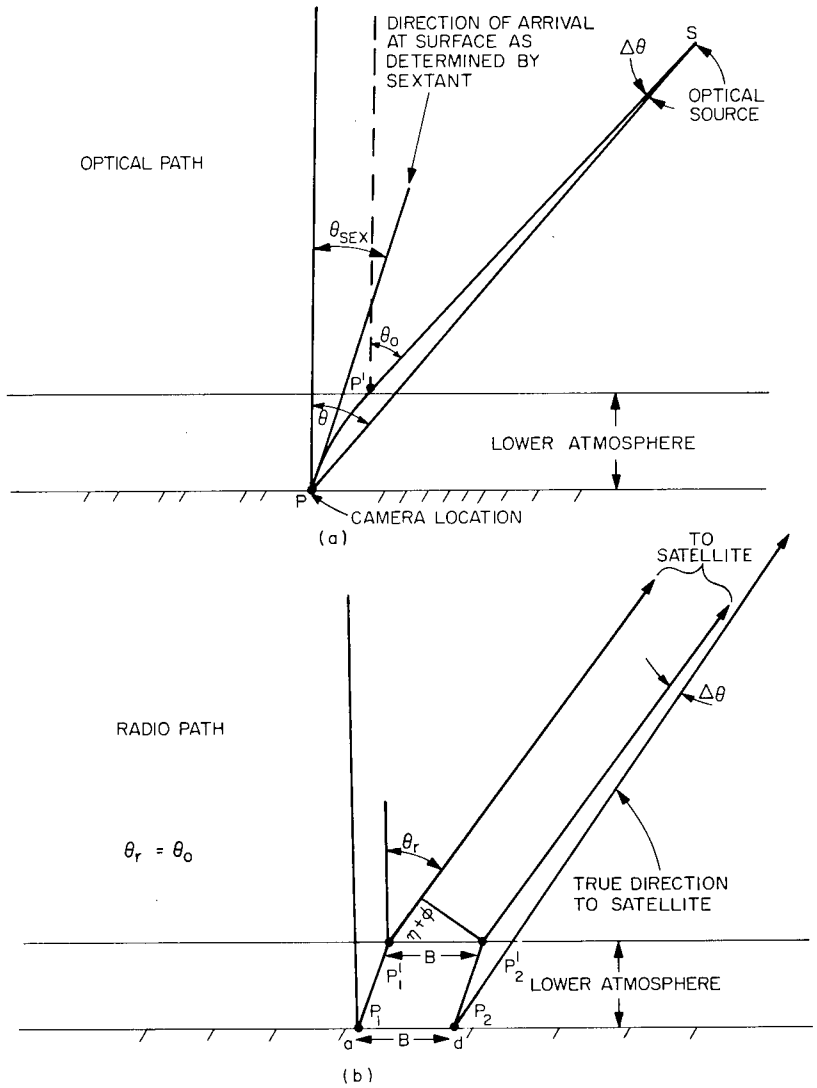

Fig. 2 - Propagation paths for (a) optical and (b) radio signals reflected from objects in space. Both the true and apparent directions are indicated.

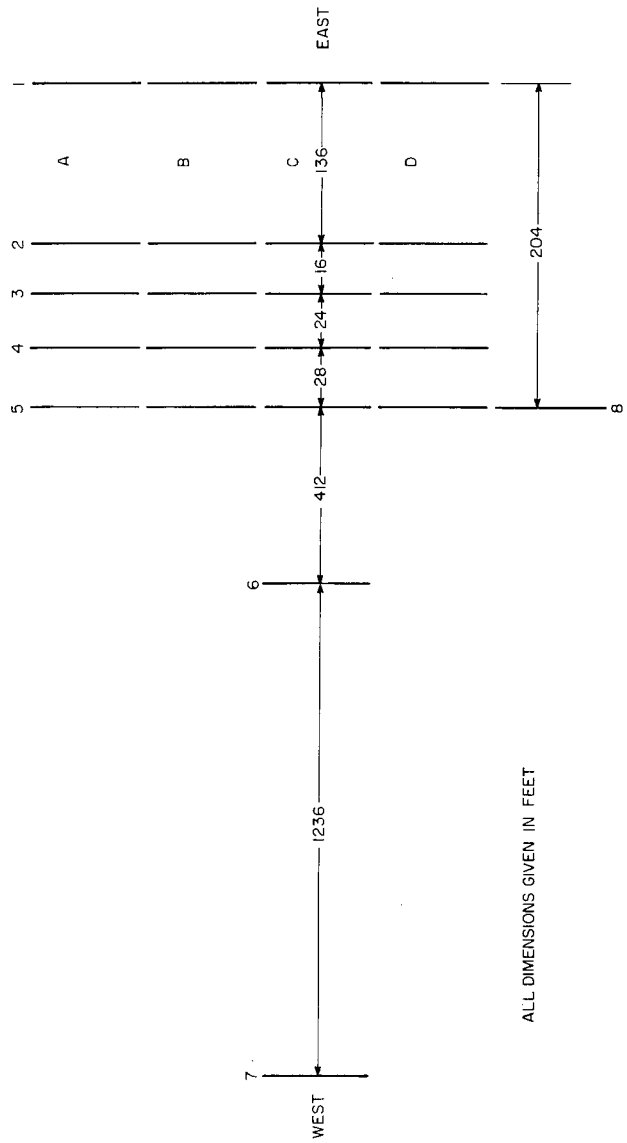

(a)

Fig. 3(a) - Receiving station antenna layout at Ft. Stewart, Ga., for 108-MHz signal reception

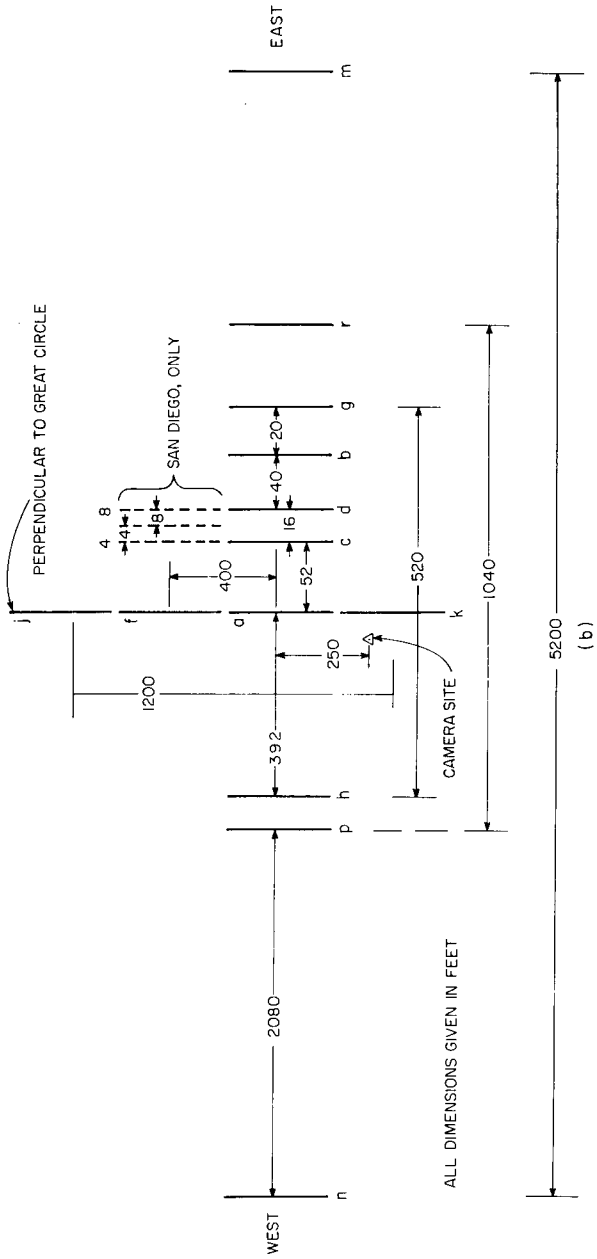

Fig. 3(b) - Receiving station antenna layout at Silver Lake, Miss., Elephant Butte, N.M., and San Diego, Calif., for 108-MHz signal reception

UNCLASSIFIED

ELECTRONIC PHASE-MEASURING EQUIPMENT

A set of electronic equipment is required for measuring the value of ϕ for each pair of baselines (1,4). The block diagram in Fig. 4 shows the arrangement for a single pair of antennas. Certain subdivisions of the receiving system offer an opportunity to partially separate variables of the system. Such a breakdown is as follows:

1. region external to the antennas (troposphere, ionosphere, and terrestrial environments),
2. antenna system,
3. lines from antennas to calibration points,
4. calibration lines,
5. calibration points to hybrid junction,
6. hybrid junction to phase meter,
7. phase meter to recorder.

Recently it has been possible to obtain additional calibration information from the output of an Analog Phase-Channel Combiner (7-9) which synthesizes outputs from the various systems of electronics, such as Fig. 4, in terms of 4, 40, and 400-ft equivalent baselines.

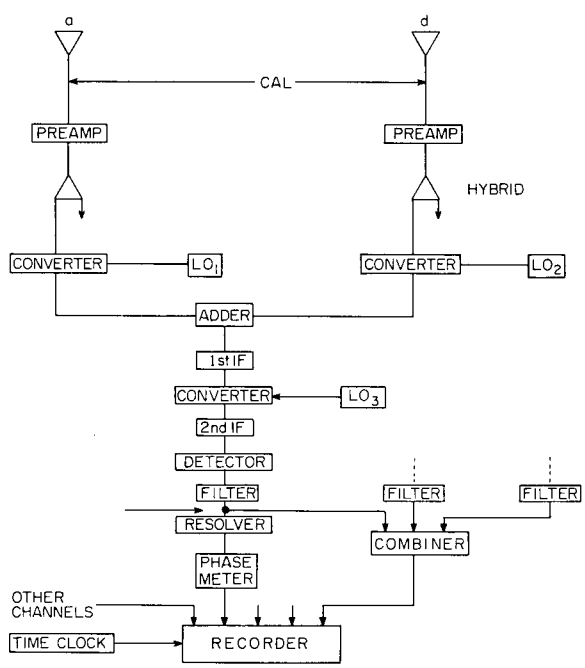

Fig. 4 - Block diagram of electronic equipment used to measure the phase difference ϕ between a pair of antennas

SYSTEM OUTPUTS

Figure 5 shows the phase output of six antenna-pair systems of the type shown in Fig. 4. The recorder pens respond to random noise when no satellite is near the xz plane (or fence). As the satellite crosses the fence, a rise in agc voltage (channel 1) is observed. Simultaneously, quieting of the phase noise in the six phase-measuring channels (channels 3-8) is observed. (Channel 2 of this record monitors the shutter voltage of the camera which photographed the satellite trail.) Figure 6 (the companion photograph to Fig. 5) shows the trail of the Echo I satellite among the stars. Time at points along the satellite trail can be identified by reference to the shutter coding on Fig. 6. This path defines the position of the satellite among the stars as a function of time. A time function is obtained by measuring the star and satellite trail positions with a comparator engine and then converting the data by means of a computer to the angular coordinates of the satellite with respect to the station from which the photograph was taken. Outputs of the program give values of θ for fence crossing time, the direction angles $\alpha(t)$ and $\beta(t)$, and their respective time derivatives. The time obtained from photographic data is located on the phase recording, and the phase values for the various baselines are read for that time. This procedure provides a set of ϕ_i's and ω_j's which are associated with the value θ_o.

REVIEW OF EARLIER OPTICAL CALIBRATION

The initial optical calibration of the Space Surveillance system has been presented in NRL Report 5741 (Ref. 3) which treated data on baselines from 16 ft to 520 ft. Measurements of error in the north-south direction were beyond the capability of the method used at that time. Measurable errors were detected in the east-west baselines. It was shown that a plot, for each fence crossing, of the form

$$\Delta\theta(\theta) = \theta_r - \theta_o \tag{16}$$

leads to a nonlinear function of the zenith angle. However, a plot of

$$\Delta(\sin\theta) = \sin\theta_r - \sin\theta_o \tag{17}$$

was independent of the zenith angle to the satellite. It was feasible, therefore, to plot $\Delta(\sin\theta)$ as a function of calendar date. This latter procedure immediately revealed a step jump in calibration error at one of the stations. Further, the bias errors observed in the data could be attributed to errors in the effective length of the transmission lines. A degree of randomness remained in the data, in addition to the bias error, which was considered due to one or more of the following possibilities:

1. random shifts in phase-measuring equipment,
2. random errors in reading data,
3. random variations in direction of arrival of radio signals,
4. random errors in optical angle measurements.

The first two possibilities represent errors entering directly in the value ϕ, and the second two enter in the value of θ. Consideration of the equation

$$\delta\phi = B\delta(\sin\theta) \tag{18}$$

allowed us to note that errors in $\delta\phi$, due to errors entering through θ, approach zero linearly as B approaches zero. It was shown that, as a consequence of this relationship,

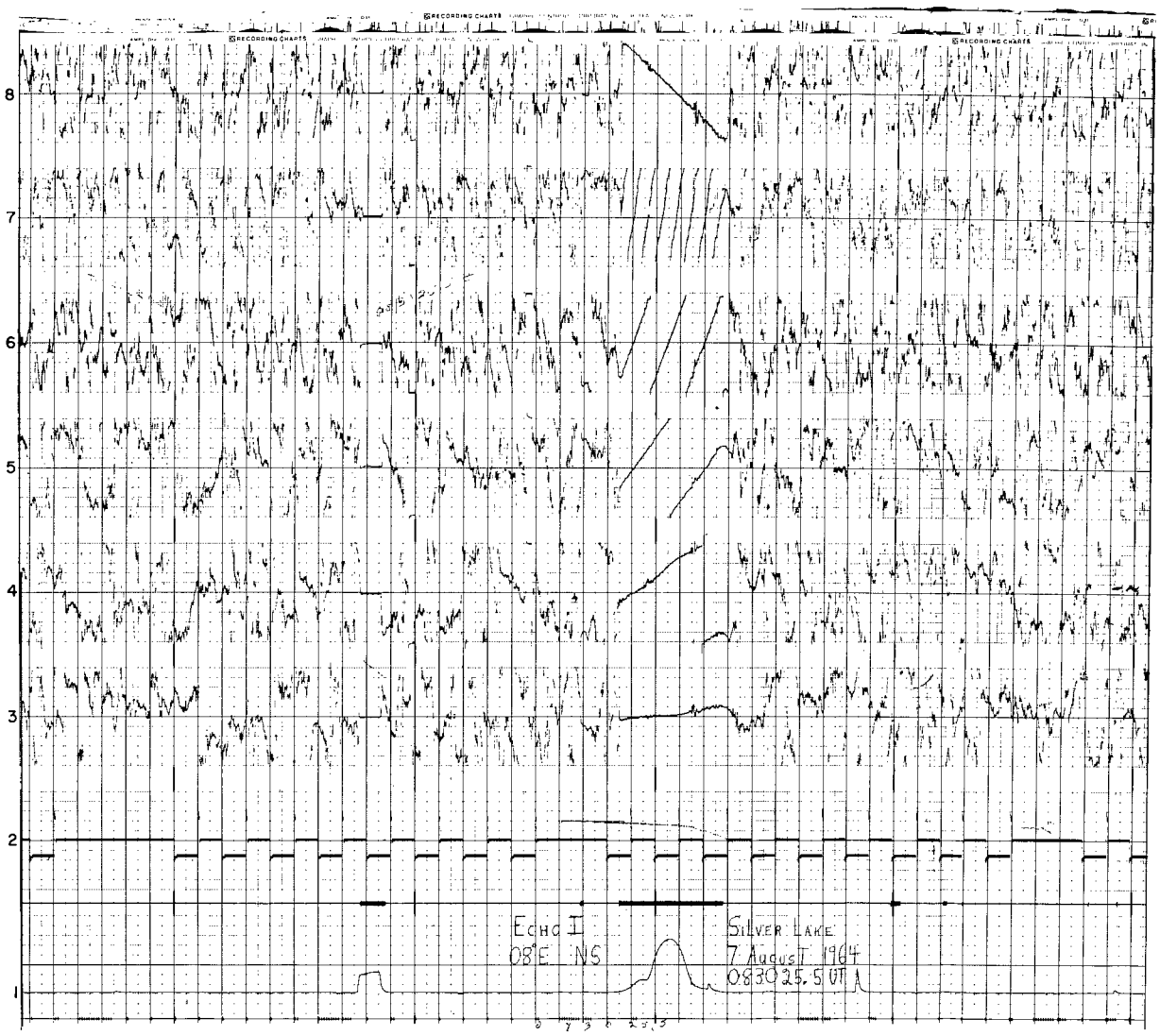

Fig. 5 - Typical phase output from six antenna-pair systems (channels 3-8) for a satellite passage. Channel 1 shows the agc voltage and channel 2 displays the shutter voltage of the camera which photographed the satellite trail (see Fig. 6). These outputs are for passage of the Echo I satellite through the "fence" on August 7, 1964, 083025.5 UT.

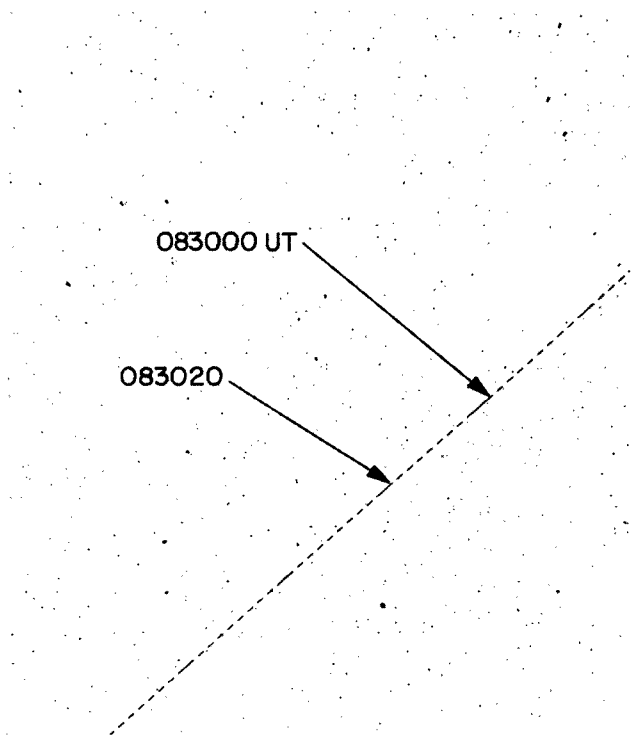

Fig. 6 - Echo I satellite pass photographed on August 7, 1964 (see Fig. 5 for electronic system outputs)

$\delta\phi$ contained an error that was inherently associated with ϕ and equal to $\pm 0.04\lambda$, which set a limit of ± 0.04 degree at the zenith to the precision of a system with a 520-ft baseline. It was computed from an increase in standard deviation on 520-ft baselines that the variation in the value of θ was ± 0.06 degree.* At Ft. Stewart, Georgia, where better optical equipment was in use, $\delta\phi$ was found to be independent of baseline length, indicating that fluctuations in phase due to the transmission path were not limiting the precision of the longest baseline then in use (413 ft). Hence the precision of angular measurements should continue to improve in direct proportion to baseline length.

NEW FORM OF DATA SUMMARY

The quantity $\Delta(\sin\theta)$ from Eq. (17) was used as a plotting parameter in the earlier work. However, its magnitude is inversely proportional to baseline length, requiring a wide range of scales for the various baselines considered in this report. This inconvenience has been eliminated by utilizing, for east-west baselines, the function

$$\Delta\phi_i = \phi_{ri} - \phi_{oi} + (n_{ri} - n_{oi}), \tag{19}$$

in which the equivalent phase ϕ_{oi} for the ith baseline obtained optically is

*The stations with the larger error in θ used cut film, which tended to bow out from the focal plane in the camera, defocusing the image and reducing the precision of measurement.

$$\phi_{oi} = B_i \sin \theta_o - n_i \,, \tag{20}$$

and for the north-south baselines the corresponding function is

$$\Delta\omega_j = \omega_{rj} + m_{rj} \,. \tag{21}$$

For each optically determined fence crossing at a station, the solutions of Eqs. (19) and (21) provide the errors $\Delta\phi_i$ and $\Delta\omega_j$ which have been plotted as functions of modified Julian Day* for the station. A sample of this type of plot (Fig. 7) shows the $\Delta\phi$'s for a few baselines at Elephant Butte, N.M., over a limited period of time. A bias error and a random-type error are apparent. A breakdown occurred on the 520-ft baseline during the period covered by this plot; it is the only event of that type detected during optical calibration. Bias changes and increased dispersion of data points for the 1040, 2080, and 5200-ft baselines are apparent. (A small change occurred also in the bias on the 520-ft baseline from before to after the breakdown.) Plots similar to Fig. 7 have been made for all baselines but are too bulky to include in this report. Instead, summaries of such data are given in Tables 1 through 4,† which include mean values of $\Delta\phi$ and $\Delta\omega$, standard deviation, and standard deviation in the mean values of $\Delta\phi$ and $\Delta\omega$ for periods between bias changes.

A summary of the number of bias changes for each baseline during the period of this report is given in Table 5. No bias changes were recorded on baselines of 520 ft or less at the San Diego and Silver Lake‡ stations; only one change occurred at Ft. Stewart (the change was associated with a change of 1 ft in the baseline length). At Elephant Butte, one change took place in the bias for all baselines due to a general rephasing of the system, in addition to the small changes associated with the breakdown mentioned above. Changes in bias for the north-south baselines have also been rare. Hence, bias errors for these baselines can be accurately determined by optical calibration and extracted by a calibration correction to output data.

Figure 8 is a plot of bias errors for the baselines of 520 ft or less at the four receiving stations. The mean calibration error for San Diego, Elephant Butte, and Silver Lake is $-0.006 \pm 0.032\lambda$. This measurement supplies a figure for accuracy (bias) and precision (scatter of measurements) which was obtained with the electronic measuring devices then in use. The corresponding calibration error for Ft. Stewart is $-0.056 \pm 0.054\lambda$, which is noticeably inferior to the figures for the other three stations. The larger errors were probably due to the increased bias errors on the 136 through 412-ft baselines at that station.

Calibration errors for baselines longer than 520 ft are given in Tables 1-4, inclusive, and are plotted in Figs. 9(a)-(d). The sets of calibration errors existing at a station at a particular time are connected by broken lines and numbered in chronological order. These errors are generally large in terms of a wavelength. There is some indication that the initial calibration errors had a dependence of the form

$$y = mx + b + p\lambda/2 \tag{22}$$

in which p is a small whole number. This dependence tends to disappear with subsequent bias adjustments. The magnitude of the bias errors have not been consistently reduced by changes which have been made in the calibration system. Since each time the bias is altered, some time is required to obtain precise optical calibration data, precise figures

*Modified Julian Day = Julian Day - 2,400,000.5 days.
†All tables are collected at the end of the report.
‡A bias shift prior to the period covered by this report occurred at Silver Lake between January 10 and 12, 1961. A corrective change was made to the baseline on June 28, 1961. (See Ref. 3.)

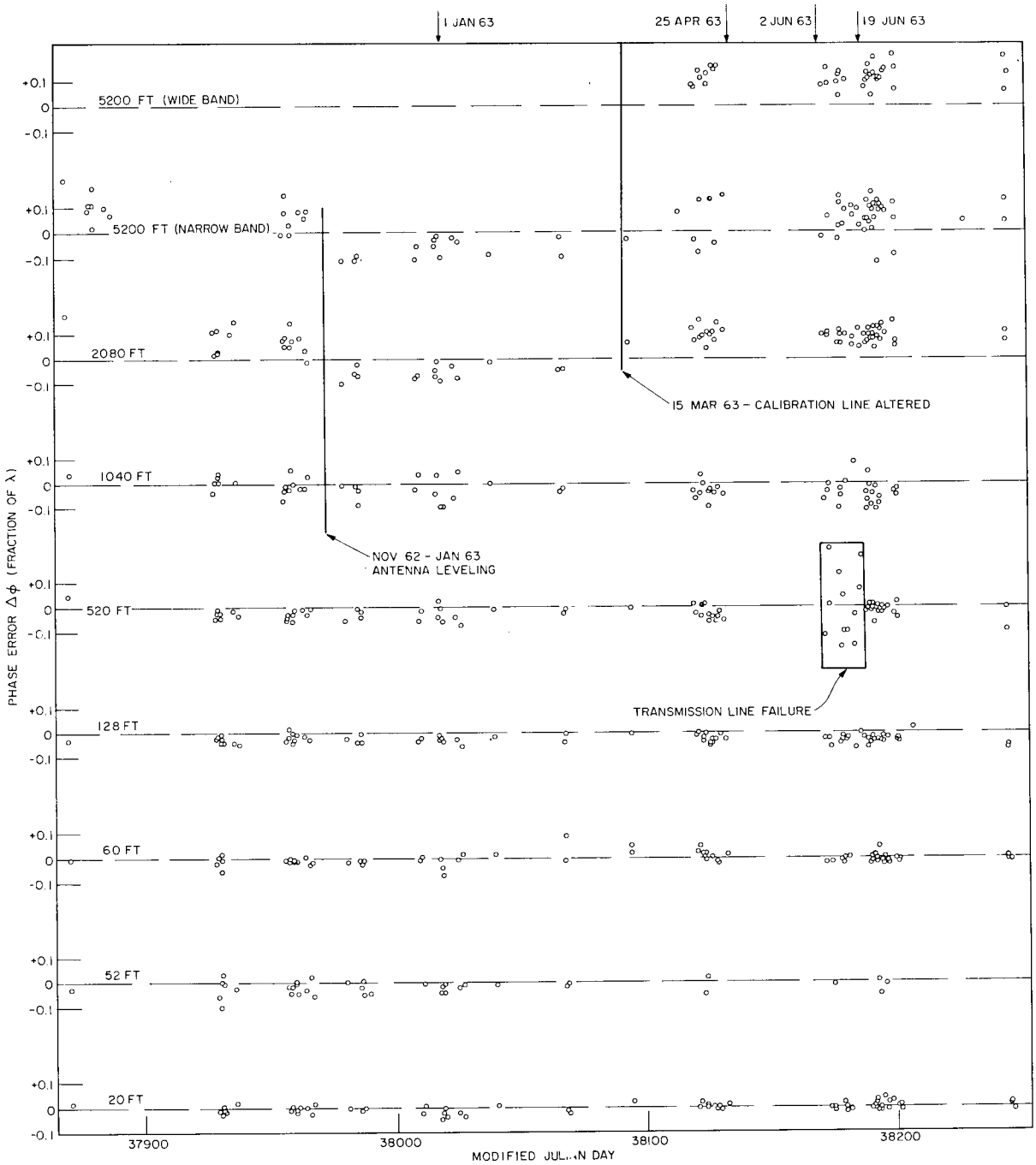

Fig. 7 - Plot of east-west-baseline phase error $\Delta\phi$ (Eq. (19)) vs time (modified Julian days) for some baselines at the Elephant Butte, N.M., station

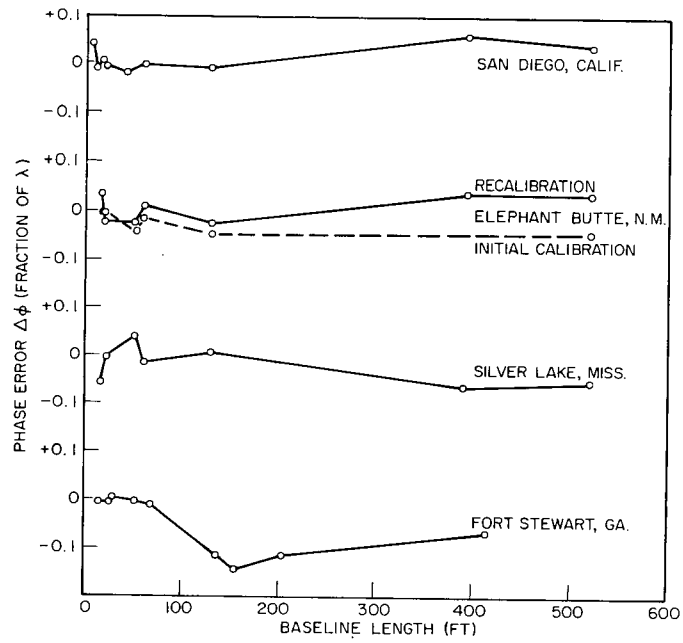

Fig. 8 - Plot of bias errors at the four receiving stations for baselines of 520 ft or less

for bias errors are not always available. This situation results in a temporary reduction in the accuracy capability of the system until new values of bias errors have been determined.

SCATTER OF POINTS

Unlike bias errors which, once determined, can be removed as calibration corrections, the random scatter of points is a more basic limitation to the system. Figure 7 shows the scatter of data points for several baselines at Elephant Butte, N.M. The histogram for one baseline at Ft. Stewart, Ga. (Fig. 10) illustrates that the distribution approximates the Gaussian normal distribution. This experimentally determined distribution supports the procedure of computing standard deviation for all baselines covered in this report, as given in Tables 1-4, along with the bias values.*

A weighted mean standard deviation for each baseline length at all the stations has been computed and the results have been plotted in Fig. 11. The points at Ft. Stewart, Georgia, have in addition been plotted separately. The standard deviation for that station tends to be constant for baselines up to about 200 ft and increases slowly to $\pm 0.08\lambda$ for the 1852-ft baseline. The standard deviations of all baselines from 16 to 520 ft appear to

*This normal distribution formula was applied to the period when the 520-ft baseline failed to resolve, giving an erroneous value of $0.010 \pm 0.261\lambda$. Reference to Fig. 7 reveals that the distribution is non-Gaussian. Since the function is multivalued at intervals of one wavelength, one is led to interpret all measured errors within the range of $\pm \lambda/2$. If the normal distribution formula is applied to a bounded distribution of this sort where there is equal probability of falling on any point within the range of $\pm \lambda/2$, one obtains $0.000 \pm 0.289\lambda$, which approximates the value given above for the period of breakdown.

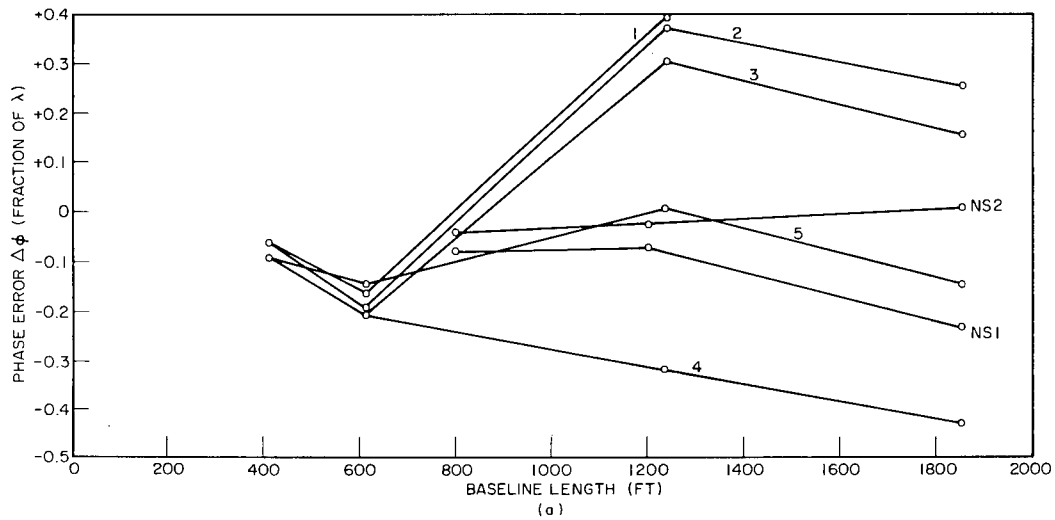

(a)

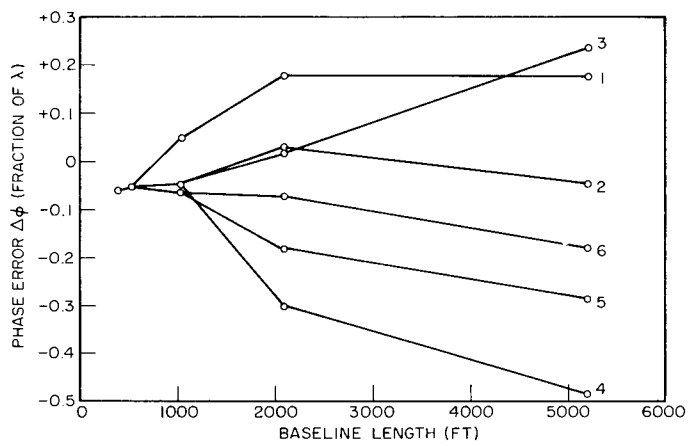

(b)

Fig. 9 - Plot of bias errors at the four receiving stations for baselines longer than 520 ft: (a) Ft. Stewart, (b) Silver Lake. The number by each baseline indicates the order in which the calibrations occurred; in the case of Ft. Stewart two calibrations on the north-south baselines are also included.

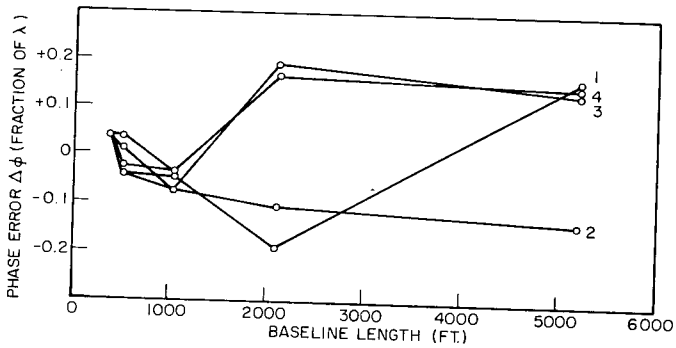

(c)

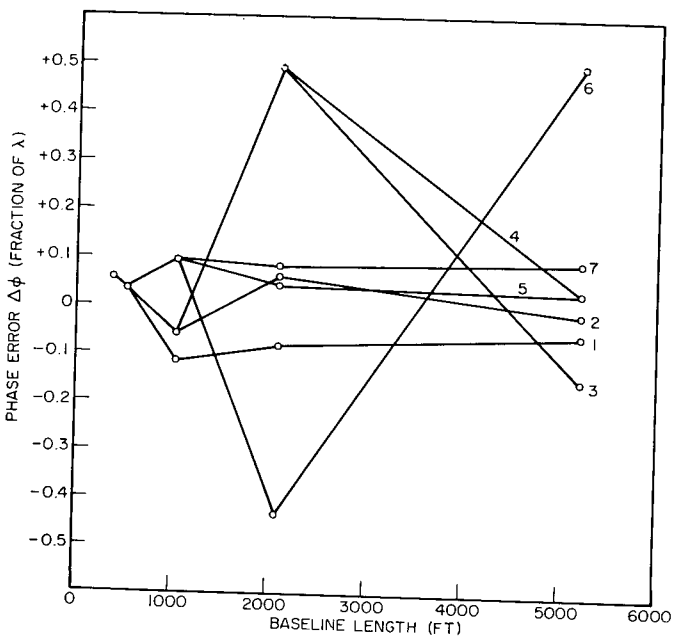

(d)

Fig. 9 - Plot of bias errors at the four receiving stations for baselines longer than 520 ft: (c) Elephant Butte, and (d) San Diego. The number by each baseline indicates the order in which the calibrations occurred.

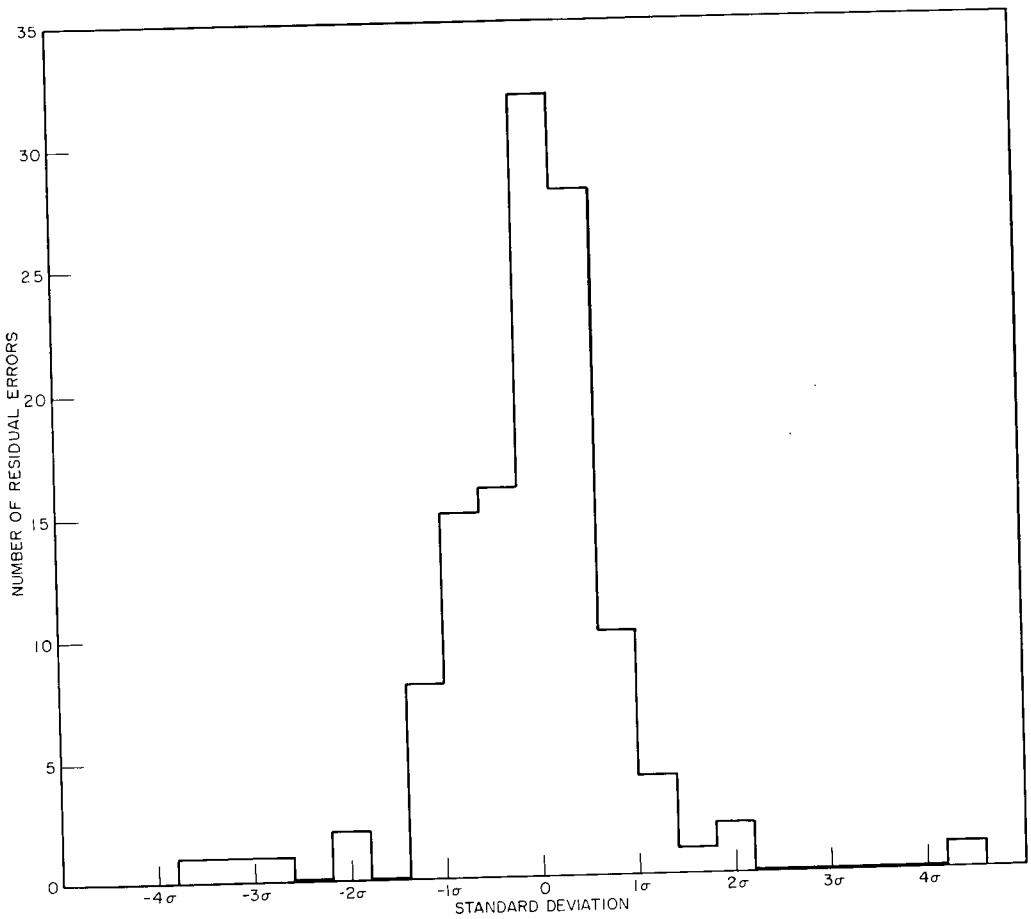

Fig. 10 - Histogram of phase error residuals for the 136-ft east-west baseline of Ft. Stewart, Ga.

be independent of baseline length and to have a weighted mean value of $\pm 0.034\lambda$. For baselines exceeding 520 ft, the standard deviation increases until it reaches $\pm 0.09\lambda$ for the 5200-ft baseline. These results provide an experimental basis for determining the probability of correctly resolving the integral parts n and m of the east-west and north-south path differences, respectively, from one baseline to the next for baselines of various lengths.*

Equation (11), which gives the limits to allowable error, must be replaced by a slightly modified formulation to provide a solution in terms of the standard deviation σ. In the special case where random errors for different baselines are uncorrelated, the standard deviation in n_{k+1} is (10)

$$\sigma(n_{k+1}) = \sqrt{\left(\frac{B_{k+1}}{B_k}\,\sigma_k\right)^2 + (\sigma_{k+1})^2}\ . \tag{23}$$

*The assumption here is that all signals will behave similarly to those of the Echo-type satellite for baselines from 16 to 520 ft.

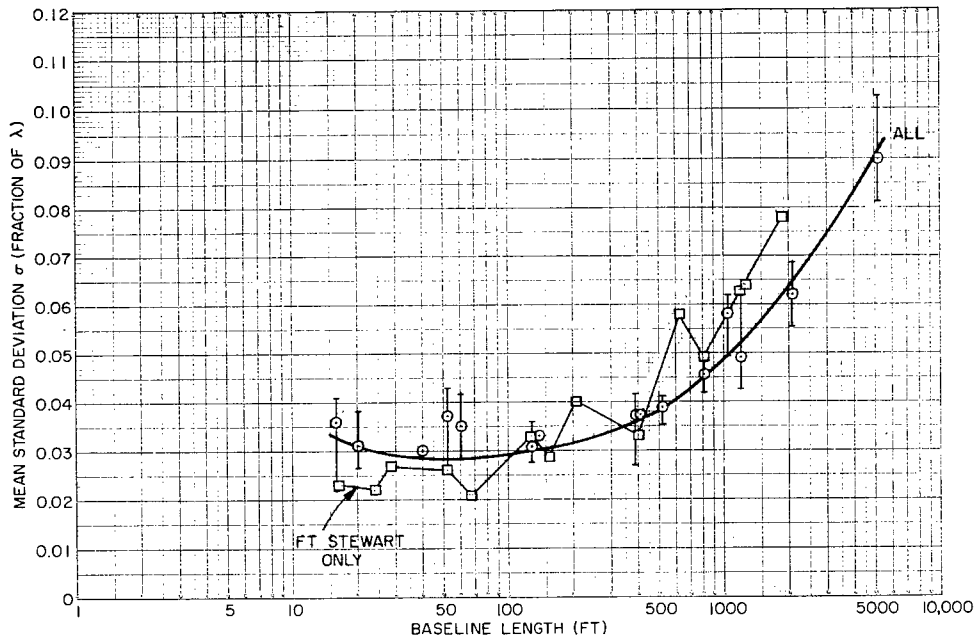

Fig. 11 - Weighted mean standard deviation vs baseline length for all receiving stations. The Ft. Stewart data is also plotted separately.

Equation (23) treats the statistical problem based on standard deviation.

Having experimental values of the standard deviation for Echo passes, the probability of correctly resolving passes which behave in a similar manner can be estimated. For such restricted cases the probability of reading n_{k+1} correctly, if n_k is correctly resolved in a system with corrections made for bias, is 99.9 percent for baselines up through 2080 ft and 99.5 percent for the 5200-ft baseline. This high percentage of correctly resolved passes necessitates accurately correcting for bias.

This is shown in the table below where percentage of correctly resolved passes are given versus bias error in the 2080-ft baseline and no uncorrected bias in other baselines.

2080-ft BL Bias (fraction of λ)	5200-ft BL Correctly Resolved Passes (percent)
0.00	99.5
0.05	98.2
0.10	91.9
0.15	75.8
0.20	50.0

The weighted mean standard deviation for the 5200-ft baseline is $\pm 0.09\lambda$, roughly 2.5 times that of the shorter baselines. This overall error on the longest baseline sets a limit to angular resolution of ±32 sec* of arc at the zenith.

*Compare this with Ref. 11.

MISCELLANEOUS TOPICS

Figure 4 shows the path of a signal received by antennas a and d which enters the recorder by two alternative paths. One is the phase recording of an individual antenna pair. The second is the combined output of two or more antenna pairs which has been converted to equivalent 4, 40, or 400-ft baselines. Ideally, the combiner channel should have a phase reading equivalent to the longest baseline included in the combiner according to the formula:

$$\text{Combiner phase error} = \left(\frac{\text{equiv. combiner baseline}}{\text{longest baseline in combiner input}}\right) \times (\text{error in longest baseline}) . \qquad (24)$$

An analysis using Eq. (24) has been made for a sample of data from the San Diego Station.* The results are as follows:

Longest baseline in combiner (ft)	Phase error of longest baseline (fraction of λ)	Predicted combiner error by Eq. (23) (fraction of λ)	Measured on recording (fraction of λ)
128	-0.007 ± 0.041	0.000 ± 0.001	$+0.007 \pm 0.036$
520	$+0.042 \pm 0.036$	$+0.003 \pm 0.003$	$+0.003 \pm 0.007$
5200	$+0.002 \pm 0.083$	0.000 ± 0.006	-0.077 ± 0.006

The figures for the 4-ft combiner ($+0.007 \pm 0.036\lambda$) is unexpectedly large. This unexpected error resulted from a procedure of having the pen travel exceed the range of the recorder paper by 12 percent. When a correction was applied for this error, the new measured value was $+0.001 \pm 0.007\lambda$, which is satisfactory agreement. The discrepancy in the measured value for the 5200-ft baseline can also be resolved in a satisfactory manner. Since the combiner error is known from optical calibration, we may insert its value ($-0.077 \pm 0.006\lambda$) into Eq. (24) and solve for the error in the 5200-ft baseline. This calculation gives a value of $-1.001 \pm 0.078\lambda$. Hence it is clear that the combiner was in error by one wavelength in terms of phase. (This error resulted from an error in the 2080-ft baseline of approximately $\lambda/2$, which was detected through optical calibration.)

The above comparison between combiner output and individual channel phase recordings has certain consequences in addition to illustrating the capability of optical calibration techniques. It indicates that the small standard deviation ($\pm 0.034\lambda$) for short baselines and the larger standard deviation observed on the 5200-ft baselines enters the system prior to the output of the postdetection filter; that the error entering after the postdetection filter is on the order of $\pm 0.005\lambda$. It is believed that nearly all of the error after the postdetection filter (which is at present negligible in comparison with other errors) is introduced by recorder drift and the limited precision with which it can be read.

Correlation may be found between bias error and phase rate (12). This correlation is illustrated by the negative shift in bias with increasing phase rate, shown in Fig. 12(a), and the positive shift of Fig. 12(b) in which phase error $\Delta\phi$ is plotted vs $\dot{\phi}$ of Eq. (12). This phase-rate dependence appears to be associated with the characteristics of the postdetection filter. An appreciable error of this type has been found for the 5200-ft

*Unpublished paper entitled "Optical Calibration of the Brown Field Space Surveillance Station," Space Surveillance Branch Technical Memorandum No. 99, Jan. 15, 1964, by L. O. Hayden and T. B. McCaskill.

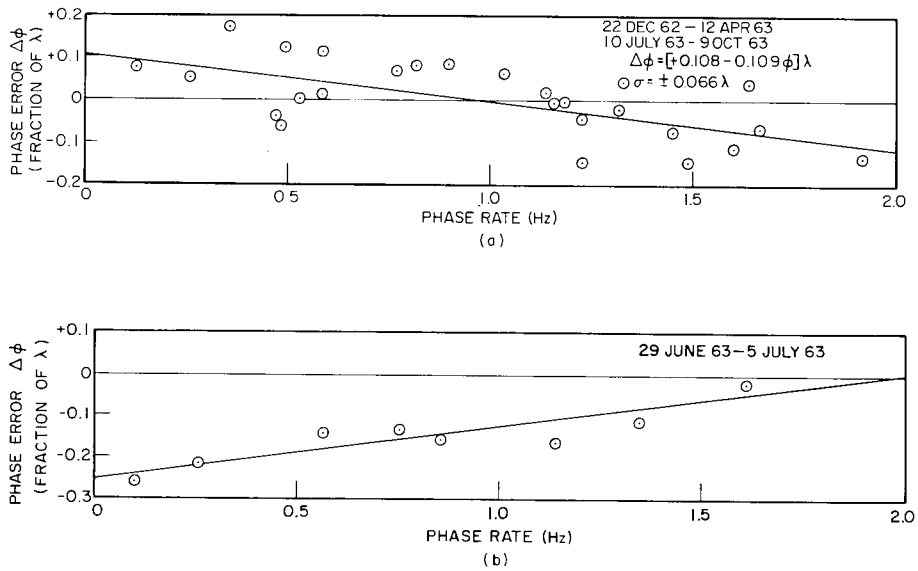

Fig. 12 - Plots of phase error $\Delta\phi$ vs phase rate $\dot{\phi}$ for the 5200-ft baseline at San Diego

baselines. Extraction of this type of error requires a determination of the phase rate for each pass to which the correction is applied.

As seen in Figs. 3 and 4 the elements of the system from the antenna to the hybrid divider (including the calibration circuits) are common to more than one baseline in many cases. If an error in the direction of arrival should exist because of ionospheric effects, a phase error proportional to the baseline length would be expected. If the shift is internal to this part of the system, it would cause an error, with either like or opposite sign, independent of baseline length.* This effect is complicated by the error in the other antenna line with which the first must be compared. This problem has been attacked by statistical methods. Table 6 gives correlation coefficients between the longest baseline in use at three receiving stations and a series of shorter baselines. Positive correlation is found with the longest and second longest baselines (which have a common element). Correlation with the next shorter baseline (which does not have a common element) is weaker. Occasional correlations show up for other baselines, but with no clear pattern. It is believed that an appreciable part of the standard deviation is due to factors external to the system, but a significant part is due to internal effects. If the known internal system errors of $\pm 0.034\lambda$ and $\pm 0.005\lambda$ are extracted, the remaining unknown error is $\pm 0.083\lambda$. This residue is an angular error, due to all unknown factors, of ± 30 sec of arc at the zenith.

In the Ft. Stewart installation, Fig. 3(a), baselines 1, 2, 3, 4, and 5 have antennas which are 1600 ft long, whereas the baselines of similar length at the other three receiving stations, Fig. 3(b), have antennas which are only 400 ft long. This difference appears to have no significant effect on the standard deviation of the baselines for signals of Echo strength.

The mean standard deviations in Fig. 11 for baselines from 616 to 1852 ft at Ft. Stewart, which are of the dipole type with ground screens, increase as a function of

*Unless it depends on calibration line length.

baseline length in amounts similar to that for the 1040, 2080, and 5200-ft baselines of the Yagi type at the three other receiving stations.

CONCLUDING REMARKS

The U.S. Navy Space Surveillance System contains a bias error which is an additive constant to the system. This error is unimportant in the shorter baselines but should be removed from the longer baselines in accordance with optical calibration data. It can be eliminated by a mathematical correction or by adjustment of the calibration lines. The latter procedure is advantageous but needs to be applied with care and full understanding of the system to avoid introducing a new calibration error which may be as bad, or worse, than the first.

A new Space Surveillance system is being built which will operate at 216 MHz to replace the system studied in this paper. Calibration data on that system will be included in a future report.

ACKNOWLEDGMENTS

The authors wish to acknowledge the guidance of Mr. R. L. Easton, Head of the Space Surveillance Branch; the consultation of Mr. C. A. Bartholomew and associates; the cooperation of contract personnel for the U.S. Naval Space Surveillance System, who furnished the photographic and recorded data essential to this report; and the personnel of the New Mexico State College, Las Cruces, New Mexico, who have reduced the photographic data.

REFERENCES

1. Easton, R. L. and Fleming, J. J., "The Navy Space Surveillance System," Proc. IRE 48(No. 4):663 (1960)

2. Berbert, J. H., Oosterhout, J. D., Engels, P. D., and Habib, E. J., "Minitrack Calibration System," Phot. Sci. Eng. 7(No. 2):78 (1963)

3. Hayden, L. O., "Optical Calibration of the U.S. Naval Space Surveillance System," NRL Report 5741, Mar. 1962

4. Mengel, J. T., "Tracking the Earth Satellite, and Data Transmission, by Radio," Proc. IRE 44(No. 6):755 (1956)

5. The American Ephemeris and Nautical Almanac, U.S. Govt. Printing Office, Washington, D.C.

6. Veis, G., "Geodetic Uses of Artificial Satellites," Smithsonian Contrib. Astrophys. 3(No. 9):95 (1960)

7. Kaufman, M. G. and Hayden, L. O., U.S. Patent No. 3,125,756 (Mar. 17, 1964)

8. Kaufman, M. G., "A Phase-Channel Combiner for the NRL Space Surveillance System," IRE Intern. Conv. Record, 10(Part 9):129 (1962)

9. Kaufman, M. G., "Radio Interferometer Phase-Channel Combiner Mod. II for the Navy Space Surveillance System," IEEE Trans. Space Electronics and Telemetry SET-10(No. 3):116 (1964)

10. Scarborough, J.B., "Numerical Mathematical Analysis," 5th ed., Baltimore:Johns Hopkins Press (1962)

11. Hendriksen, S.X., "Electronic Tracking of Artificial Satellites," p. 194 in "The Use of Artificial Satellites for Geodesy," G. Veis, ed., Amsterdam:North-Holland Publ. Co. (1963)

12. Anderson, R. L. and Bancroft, T. A., "Statistical Theory in Research," New York: McGraw-Hill (1952)

Table 1
Calibration Data for Fort Stewart, Georgia

Baseline Length (ft)	Phase Error $\Delta\phi$ Expressed as Fraction of a Wavelength			Number of Observations	Time Interval Used for Data Acquisition	
	Mean	Standard Deviation	Standard Deviation in the Mean		Calendar Dates	Modified Julian Day (MJD) Numbers*
East-West Baselines						
16	-0.007	±0.023	±0.002	83	1 Dec 61 - 25 Sept 64	37634-38693
24	-0.005	0.022	0.003	68	9 May 62 - 25 Sept 64	37793-38693
28	+0.002	0.027	0.003	72	9 May 62 - 25 Sept 64	37793-38693
52	-0.007	0.026	0.003	68	9 May 62 - 25 Sept 64	37793-38693
68	-0.010	0.021	0.003	48	2 Sept 63 - 25 Sept 64	38274-38693
136	-0.114	0.033	0.003	124	4 May 61 - 25 Sept 64	37423-38693
152	-0.142	0.029	0.012	6	7 Sept 63 - 10 Sept 63	38279-38282
204	-0.122	0.040	0.004	97	4 May 61 - 25 Sept 64	37423-38693
413	-0.064	0.034	0.004	64	4 May 61 - 16 Aug 62	37423-37892
412	-0.091	0.040	0.005	63	17 Aug 62 - 25 Sept 64	37893-38693
1234	+0.392	0.054	0.009	39	4 May 61 - 28 Dec 61	37423-37660
1234	+0.377	0.100	0.020	25	29 Dec 61 - 16 Aug 62	37661-37892
1236	+0.306	0.076	0.020	13	17 Aug 62 - 29 Oct 63	37893-38331
1236	-0.317	0.064	0.018	12	30 Oct 63 - 16 Jan 64	38332-38410
1236	+0.005	0.040	0.007	30	17 Jan 64 - 25 Sept 64	38411-38693
617	-0.164	0.043	0.007	39	4 May 61 - 28 Dec 61	37423-37660
617	-0.193	0.083	0.016	25	29 Dec 61 - 16 Aug 62	37661-37892
616	-0.204	0.069	0.015	21	17 Aug 62 - 16 Jan 64	37893-38410
616	-0.145	0.046	0.009	27	17 Jan 64 - 25 Sept 64	38411-38693
1851	+0.254	0.084	0.023	13	9 May 62 - 16 Aug 62	37793-37892
1852	+0.155	0.101	0.036	8	17 Aug 62 - 29 Oct 63	37893-38331
1852	-0.430	0.121	0.036	11	30 Oct 63 - 16 Jan 64	38332-38410
1852	-0.148	0.058	0.010	30	17 Jan 64 - 25 Sept 64	38411-38693

Table 1 (Continued)
Calibration Data for Fort Stewart, Georgia

Baseline Length (ft)	Phase Error $\Delta\phi$ Expressed as Fraction of a Wavelength			Number of Observations	Time Interval Used for Data Acquisition	
	Mean	Standard Deviation	Standard Deviation in the Mean		Calendar Dates	Modified Julian Day (MJD) Numbers*
North-South Baselines						
400	+0.001	0.033	0.003	110	4 May 61 - 25 Sept 64	37423-38693
800	-0.080	0.036	0.010	12	21 Oct 63 - 16 Jan 64	38329-38410
800	-0.041	0.054	0.010	30	17 Jan 64 - 25 Sept 64	38411-38693
1200	-0.001	0.037	0.008	19	18 Feb 62 - 16 Aug 62	37713-37892
1200	-0.070	0.062	0.011	33	17 Aug 62 - 16 Jan 64	37893-38410
1200	-0.026	0.080	0.015	30	17 Jan 64 - 25 Sept 64	38411-38693
1851	+0.325	0.068	0.019	13	9 May 62 - 16 Aug 62	37793-37892
1851	-0.230	0.061	0.015	17	17 Aug 62 - 16 Jan 64	37893-38410
1851	+0.009	0.092	0.017	30	17 Jan 64 - 25 Sept 64	38411-38693
North-South Combiners						
400	-0.016	0.023	0.005	21	22 Jan 63 - 16 Jan 64	38051-38410
400	-0.016	0.039	0.007	30	17 Jan 64 - 25 Sept 64	38411-38693
East-West Combiners						
4	-0.005	0.013	0.003	14	10 Sept 63 - 16 Jan 64	38282-38410
4	-0.004	0.010	0.002	29	17 Jan 64 - 25 Sept 64	38411-38693

*MJD = JD - 2,400,000.5 days.

UNCLASSIFIED

Table 2
Calibration Data for Silver Lake, Mississippi*

Baseline Length (ft)	Phase Error $\Delta\phi$ Expressed as Fraction of a Wavelength			Number of Observations	Time Interval Used for Data Acquisition	
	Mean	Standard Deviation	Standard Deviation in the Mean		Calendar Dates	Modified Julian Day (MJD) Numbers†
East-West Baselines						
16	-0.054	±0.040	±0.004	112	9 May 62 - 31 Oct 64	37793-38699
20	-0.001	0.027	0.003	112	24 Nov 61 - 31 Oct 64	37627-38699
52	+0.039	0.043	0.004	114	24 Nov 61 - 31 Oct 64	37627-38699
60	-0.018	0.029	0.003	114	24 Nov 61 - 31 Oct 64	37627-38699
128	+0.003	0.033	0.003	126	24 Nov 61 - 31 Oct 64	37627-38699
392	-0.061	0.038	0.004	113	20 Apr 62 - 31 Oct 64	37774-38699
520	-0.055	0.038	0.003	125	24 Nov 61 - 31 Oct 64	37627-38699
1040	+0.044	0.044	0.009	22	2 Jul 62 - 21 Nov 62	37847-37989
1040	-0.048	0.063	0.009	53	22 Nov 62 - 3 Jun 64	37990-38549
1040	-0.065	0.051	0.009	32	4 Jun 64 - 31 Oct 64	38550-38699
2080	+0.177	0.068	0.012	33	2 Jul 62 - 21 Nov 62	37847-37989
2080	+0.024	—	—	2	22 Nov 62 - 26 Nov 62	37990-37994
2080	+0.021	0.072	0.012	39	27 Nov 62 - 9 Jan 64	37995-38403
2080	-0.303	0.066	0.017	15	10 Jan 64 - 3 Jun 64	38404-38549
2080	-0.185	0.093	0.030	10	4 Jun 64 - 21 Jul 64	38550-38597
2080	-0.071	0.055	0.012	22	22 Jul 64 - 31 Oct 64	38598-38699
5200	+0.176	0.151	0.026	34	9 May 62 - 21 Nov 62	37793-37989
5200	-0.049	—	—	2	22 Nov 62 - 26 Nov 62	37990-37994
5200	+0.234	0.099	0.016	39	27 Nov 62 - 9 Jan 64	37995-38403
5200	-0.448	0.079	0.020	15	10 Jan 64 - 3 Jun 64	38404-38549
5200	-0.288	0.157	0.050	10	4 Jun 64 - 21 Jul 64	38550-38597
5200	-0.180	0.102	0.022	22	22 Jul 64 - 31 Oct 64	38598-38699

Table 2 (Continued)
Calibration Data for Silver Lake, Mississippi*

Baseline Length (ft)	Phase Error $\Delta\phi$ Expressed as Fraction of a Wavelength			Number of Observations	Time Interval Used for Data Acquisition	
	Mean	Standard Deviation	Standard Deviation in the Mean		Calendar Dates	Modified Julian Day (MJD) Numbers†
East-West Combiners						
4	-0.003	0.011	0.002	28	7 Jul 64 - 31 Oct 64	38583-38699
40	-0.010	0.008	0.001	28	7 Jul 64 - 31 Oct 64	38583-38699
400	-0.016	0.015	0.003	27	7 Jul 64 - 31 Oct 64	38583-38699
North-South Baseline						
1200	+0.004	0.043	0.004	124	24 Nov 61 - 31 Oct 64	37627-38699
North-South Combiner						
400	0.000	0.023	0.004	29	7 Jul 64 - 31 Oct 64	38583-38699

*Antennas leveled 22 Nov. 62 (MJD = 37990); 0.1λ change in the 2080 and 5200-ft baselines on 26 Nov. 62 (MJD = 37994).
†MJD = JD - 2,400,000.5 days.

UNCLASSIFIED

Table 3
Calibration Data for Elephant Butte, New Mexico*

Baseline Length (ft)	Phase Error $\Delta\phi$ Expressed as Fraction of a Wavelength			Number of Observations	Time Interval Used for Data Acquisition	
	Mean	Standard Deviation	Standard Deviation in the Mean		Calendar Dates	Modified Julian Day (MJD) Numbers†
East-West Baselines						
16	+0.000	±0.044	±0.005	82	9 May 62 - 1 Apr 64	37793-38486
16	+0.032	0.036	0.005	58	2 Apr 64 - 5 Sept 64	38487-38643
20	-0.003	0.031	0.003	83	28 Oct 61 - 1 Apr 64	37600-38486
20	-0.021	0.034	0.004	58	2 Apr 64 - 5 Sept 64	38487-38643
52	-0.042	0.049	0.007	49	28 Oct 61 - 1 Apr 64	37600-38486
52	-0.026	0.028	0.004	58	2 Apr 64 - 5 Sept 64	38487-38643
60	-0.017	0.040	0.005	62	28 Oct 61 - 1 Apr 64	37600-38486
60	+0.010	0.044	0.006	58	2 Apr 64 - 5 Sept 64	38487-38643
128	-0.048	0.031	0.003	89	28 Oct 61 - 1 Apr 64	37600-38486
128	-0.023	0.023	0.003	59	2 Apr 64 - 5 Sept 64	38487-38643
392	+0.037	0.031	0.004	59	19 Apr 64 - 5 Sept 64	38504-38643
520	-0.043	0.049	0.006	58	28 Oct 61 - 24 Apr 63	37600-38143
520	(+0.010)	(0.261)	(0.075)	12	25 Apr 63 - 19 Jun 63	38144-38199‡
520	-0.029	0.046	0.010	22	20 Jun 63 - 1 Apr 64	38200-38486
520	+0.034	0.032	0.004	59	2 Apr 64 - 5 Sept 64	38487-38643
1040	-0.044	0.061	0.011	29	14 Apr 62 - 16 Nov 62	37768-37984
1040	-0.074	0.083	0.011	54	17 Nov 62 - 1 Apr 64	37985-38486
1040	-0.040	0.043	0.006	59	2 Apr 64 - 5 Sept 64	38487-38486
2080	-0.190	0.112	0.020	30	14 Apr 62 - 16 Nov 62	37768-37984
2080	-0.106	0.053	0.014	15	17 Nov 62 - 14 Mar 63	37985-38100
2080	+0.191	0.062	0.009	48	15 Mar 63 - 1 Apr 64	38101-38486
2080	+0.167	0.061	0.008	58	2 Apr 64 - 5 Sept 64	38487-38643

Table 3 (Continued)
Calibration Data for Elephant Butte, New Mexico*

Baseline Length (ft)	Phase Error $\Delta\phi$ Expressed as Fraction of a Wavelength			Number of Observations	Time Interval Used for Data Acquisition	
	Mean	Standard Deviation	Standard Deviation in the Mean		Calendar Dates	Modified Julian Day (MJD) Numbers†
Narrow Band						
5200	+0.160	0.105	0.021	26	14 Apr 62 - 16 Nov 62	37768-37984
5200	-0.134	0.070	0.018	15	17 Nov 62 - 14 Mar 63	37985-38100
5200	+0.133	0.113	0.018	41	15 Mar 63 - 1 Apr 64	38101-38486
5200	+0.144	0.080	0.010	58	2 Apr 64 - 5 Sept 64	38487-38643
Wide Band						
5200	+0.237	0.081	0.013	37	12 Apr 63 - 1 Apr 64	38131-38486
5200	+0.177	0.064	0.009	56	2 Apr 64 - 5 Sept 64	38487-38643
East-West Combiners						
4	+0.003	0.010	0.001	57	19 Apr 64 - 5 Sept 64	38504-38643
40	+0.002	0.013	0.002	48	19 Apr 64 - 5 Sept 64	38504-38643
400	+0.004	0.015	0.002	47	19 Apr 64 - 5 Sept 64	38504-38643
North-South Baselines						
400	-0.010	0.035	0.005	58	19 Apr 64 - 5 Sept 64	38504-38643
800	-0.009	0.046	0.006	58	19 Apr 64 - 5 Sept 64	38504-38643
1200	+0.006	0.047	0.005	89	28 Oct 61 - 1 Apr 64	37600-38486
1200	-0.015	0.064	0.008	57	2 Apr 64 - 5 Sept 64	38487-38643
North-South Combiner						
400	-0.001	0.022	0.003	56	19 Apr 64 - 5 Sept 64	38504-38643

*Antennas leveled 16 Nov. 62 (MJD = 37984); 0.17λ change in the 2080 and 5200-ft baselines on 15 Mar. 63 (MJD = 38101); primary calibration adjustment on 2 Apr. 64 (MJD = 38487).
†MJD = JD - 2,400,000.5 days.
‡See discussion in section on "New Form of Data Summary."

UNCLASSIFIED

Table 4
Calibration Data for San Diego, California*

Baseline Length (ft)	Phase Error $\Delta\phi$ Expressed as Fraction of a Wavelength			Number of Observations	Time Interval Used for Data Acquisition	
	Mean	Standard Deviation	Standard Deviation in the Mean		Calendar Dates	Modified Julian Day (MJD) Numbers†
East-West Baselines						
4	+0.041	±0.044	±0.007	41	29 Jun 63 - 3 Sept 64	38209-38641
8	-0.010	0.059	0.008	59	28 Dec 62 - 3 Sept 64	38026-38641
16	+0.004	0.035	0.005	55	14 Apr 62 - 3 Sept 64	37768-38641
20	-0.004	0.038	0.005	66	26 Jan 62 - 3 Sept 64	37690-38641
40	-0.022	0.030	0.011	20	14 Apr 64 - 3 Sept 64	38499-38641
60	-0.002	0.034	0.004	67	26 Jan 62 - 3 Sept 64	37690-38641
128	-0.010	0.036	0.005	59	26 Jan 62 - 3 Sept 64	37690-38641
392	+0.060	0.042	0.007	39	29 Jun 63 - 3 Sept 64	38209-38641
520	+0.037	0.036	0.004	70	26 Jan 62 - 3 Sept 64	37690-38641
1040	-0.119	0.066	0.025	7	11 Apr 62 - 18 Nov 62	37765-37986‡
1040	-0.058	0.045	0.010	21	19 Nov 62 - 3 Jan 64	37987-38397
1040	+0.093	0.054	0.011	24	4 Jan 64 - 3 Sept 64	38398-38641
2080	-0.089	0.255	0.100	7	11 Apr 62 - 18 Nov 62	37765-37986‡
2080	+0.060	0.045	0.011	18	19 Nov 62 - 12 Apr 63	37987-38131
2080	+0.491	0.064	0.015	18	29 Jun 63 - 3 Jan 64	38209-38397§
2080	+0.041	—	—	1	4 Jan 64 - 15 Jan 64	38398-38409
2080	-0.434	0.066	0.017	16	12 Apr 64 - 20 May 64	38497-38535¶
2080	+0.082	0.038	0.015	6	21 May 64 - 3 Sept 64	38536-38641
5200	-0.060	0.332	0.125	7	11 Apr 62 - 18 Nov 62	37765-37986
5200	-0.015	0.075	0.018	18	19 Nov 62 - 12 Apr 63	37987-38131**
5200	-0.155	0.064	0.023	8	29 Jun 63 - 5 Jul 63	38209-38215
5200	+0.030	0.078	0.023	11	10 Jul 63 - 12 Jan 64	38220-38406
5200	-0.343	—	—	1	13 Jan 64 - 15 Jan 64	38407-38409
5200	+0.499	0.109	0.027	16	12 Apr 64 - 20 May 64	38497-38535††
5200	+0.091	0.087	0.035	6	21 May 64 - 3 Sept 64	38536-38641‡‡,§§

Table 4 (Continued)
Calibration Data for San Diego, California*

Baseline Length (ft)	Phase Error $\Delta\phi$ Expressed as Fraction of a Wavelength			Number of Observations	Time Interval Used for Data Acquisition	
	Mean	Standard Deviation	Standard Deviation in the Mean		Calendar Dates	Modified Julian Day (MJD) Numbers†
East-West Combiners						
4	+0.001	0.007	0.002	16	16 Mar 63 - 13 Jul 63	38104-38223
4	+0.003	0.008	0.001	30	30 Sept 63 - 3 Sept 64	38302-38641
40	+0.004	0.007	0.001	37	29 Jun 63 - 3 Sept 64	38209-38641
400	-0.080	0.014	0.004	13	29 Jun 63 - 12 Jan 64	38209-38406
400	+0.028	—	—	1	13 Jan 64 - 9 Mar 64	38407-38463
400	+0.006	0.020	0.006	9	10 Mar 64 - 20 May 64	38464-38535
400	+0.012	0.012	0.005	6	21 May 64 - 3 Sept 64	38536-38641
North-South Baselines						
400	+0.003	0.027	0.005	32	10 Sept 63 - 3 Sept 64	38282-38641
800	+0.056	0.042	0.007	32	10 Sept 63 - 3 Sept 64	38282-38641
1200	+0.017	0.041	0.005	67	11 Apr 62 - 3 Sept 64	37765-38641
North-South Combiner						
400	+0.002	0.013	0.003	20	29 Jun 63 - 3 Sept 64	38209-38641

*Frequency changed from 108 to 108.015 Mc/s on 28 and 29 Dec. 61 (MJD = 37660 and 37661).
†MJD = JD - 2,400,000.5 days.
‡Antennas leveled on 19 Nov. 62 (MJD = 37987).
§Exact date of change which occurred between 12 Apr. 63 and 29 June 63 (MJD = 38131 to 38209) is not known.
¶The 1040 and 2080-ft baselines were rephased on 4 Jan. 64 (MJD = 38398).
**The 1040, 2080, and 5200-ft baselines were rephased on 13 Jan. 64 (MJD = 38407).
††New cable was installed in all long baselines on 10 Mar. 64 (MJD = 38464).
‡‡Half wavelength was added to 2080 and 5200-ft baselines on 21 May 64 (MJD = 38536).
§§The 5200-ft-baseline cable change was completed on 2 Oct. 64 (MJD = 38670).

UNCLASSIFIED

Table 5
Number of Shifts in Bias ($\Delta\phi$) During Period of Observation

Baseline Length (ft)	Number of Shifts for the Station Indicated				
	Silver Lake	Elephant Butte	San Diego	Fort Stewart	
East-West Baseline				East-West Baseline	
4	-	-	0		
8	-	-	0	16	0
16	0	1	0	24	0
20	0	1	0	28	0
40	-	-	0	52	0
52	0	1	-	68	0
60	0	1	0	136	0
128	0	1	0	152	0
392	0	0	0	204	0
520	0	3	0	413/2	1
1040	2	2	2	1234/6	4
2080	5	3	5	617/6	3
5200	5	3	6	1851/2	3
North-South Baseline				North-South Baseline	
400	-	0	0	400	0
800	-	0	0	800	1
1200	0	1	0	1200	2
1851	-	-	-	1851	2

Table 6
Correlation of Longest Baseline with Shorter Baselines at Each of Three Stations

Correlation of								
Ft. Stewart, Ga. 1852-ft BL with			Silver Lake, Miss. 5200-ft BL with			Elephant Butte, N.M. 5200-ft BL with		
BL (ft)	r*	N	BL (ft)	r	N	BL (ft)	r	N
1236	0.745	27	2080	0.666	22	2080	0.530	55
616	0.514	27	1040	0.269	22	1040	0.491	55
412	0.198	27	520	0.265	22	520	0.307	55
204	0.105	27	392	0.114	22	392	0.095	55
136	0.227	27	128	-0.348	22	128	0.175	55
28	0.242	27	60	-0.416	22	60	0.016	55
24	0.286	27	52	0.062	22	52	0.370	55
			20	-0.193	22	20	0.020	55
			16	-0.260	22	16	-0.142	55

*The correlation factor $r = \dfrac{\sum_{i=1}^{N} r_x r_y}{N \sigma_x \sigma_y}$,

where $r_x = x_i - \bar{x}$, $r_y = y_i - \bar{y}$.

Security Classification

DOCUMENT CONTROL DATA - R&D

(Security classification of title, body of abstract and indexing annotation must be entered when the overall report is classified)

1. ORIGINATING ACTIVITY *(Corporate author)*

U.S. Naval Research Laboratory
Washington, D.C. 20390

2a. REPORT SECURITY CLASSIFICATION

UNCLASSIFIED

2b. GROUP

3. REPORT TITLE

OPTICAL CALIBRATION ANALYSIS OF THE U.S. NAVAL SPACE SURVEILLANCE SYSTEM

4. DESCRIPTIVE NOTES *(Type of report and inclusive dates)*

A final report on one phase of the problem.

5. AUTHOR(S) *(Last name, first name, initial)*

Hayden, L. O., and McCaskill, T. B.

6. REPORT DATE

April 25, 1966

7a. TOTAL NO. OF PAGES

36

7b. NO. OF REFS

12

8a. CONTRACT OR GRANT NO.

NRL Problem R02-35

b. PROJECT NO.

RT 8801-001/6521/S434-00-01

c.

d.

9a. ORIGINATOR'S REPORT NUMBER(S)

NRL Report 6385

9b. OTHER REPORT NO(S) *(Any other numbers that may be assigned this report)*

None

10. AVAILABILITY/LIMITATION NOTICES

Distribution of this document is unlimited. Copies available from the Clearinghouse for Scientific and Technical Information (CFSTI), Springfield, Va., 22151

11. SUPPLEMENTARY NOTES

None

12. SPONSORING MILITARY ACTIVITY

Dept. of the Navy (Bureau of Weapons)

13. ABSTRACT

A preliminary optical calibration of the U.S. Naval Space Surveillance System was made in 1961 using graphical methods. Since then, calibration has been continued using better equipment and data reduction methods to determine more precisely the characteristics of the system. It is shown that the 108-MHz system studied is capable of measuring angles within a standard deviation σ of 1/2 min of arc at zenith.

Electronic calibration methods used in setting up the 108-MHz system are shown to have a mean accuracy of approximately 3.5 percent of a wavelength for baselines up through 520 ft in length. Bias errors for baselines of 1040 ft and longer are larger than for the shorter baselines and must be corrected to obtain maximum accuracy from the system.

Baselines in the range of 16 to 520 ft have (for Echo passes) a mean standard deviation of $\pm 0.034\lambda$, which is independent of baseline length and angle of arrival and is internal to the system. The random error for longer baselines increases until it reaches a mean standard deviation of $\pm 0.09\lambda$ for the 5200-ft baseline.

DD FORM 1 JAN 64 1473

Security Classification

14. KEY WORDS	LINK A ROLE	LINK A WT	LINK B ROLE	LINK B WT	LINK C ROLE	LINK C WT
Space Surveillance Systems						
Navy						
Calibration						
Optics						
Angle of arrival						
Phase (electrical)						
Phase measurement						
Errors						
Statistical analysis						

INSTRUCTIONS

1. ORIGINATING ACTIVITY: Enter the name and address of the contractor, subcontractor, grantee, Department of Defense activity or other organization *(corporate author)* issuing the report.

2a. REPORT SECURITY CLASSIFICATION: Enter the overall security classification of the report. Indicate whether "Restricted Data" is included. Marking is to be in accordance with appropriate security regulations.

2b. GROUP: Automatic downgrading is specified in DoD Directive 5200.10 and Armed Forces Industrial Manual. Enter the group number. Also, when applicable, show that optional markings have been used for Group 3 and Group 4 as authorized.

3. REPORT TITLE: Enter the complete report title in all capital letters. Titles in all cases should be unclassified. If a meaningful title cannot be selected without classification, show title classification in all capitals in parenthesis immediately following the title.

4. DESCRIPTIVE NOTES: If appropriate, enter the type of report, e.g., interim, progress, summary, annual, or final. Give the inclusive dates when a specific reporting period is covered.

5. AUTHOR(S): Enter the name(s) of author(s) as shown on or in the report. Enter last name, first name, middle initial. If military, show rank and branch of service. The name of the principal author is an absolute minimum requirement.

6. REPORT DATE: Enter the date of the report as day, month, year; or month, year. If more than one date appears on the report, use date of publication.

7a. TOTAL NUMBER OF PAGES: The total page count should follow normal pagination procedures, i.e., enter the number of pages containing information.

7b. NUMBER OF REFERENCES: Enter the total number of references cited in the report.

8a. CONTRACT OR GRANT NUMBER: If appropriate, enter the applicable number of the contract or grant under which the report was written.

8b, 8c, & 8d. PROJECT NUMBER: Enter the appropriate military department identification, such as project number, subproject number, system numbers, task number, etc.

9a. ORIGINATOR'S REPORT NUMBER(S): Enter the official report number by which the document will be identified and controlled by the originating activity. This number must be unique to this report.

9b. OTHER REPORT NUMBER(S): If the report has been assigned any other report numbers *(either by the originator or by the sponsor)*, also enter this number(s).

10. AVAILABILITY/LIMITATION NOTICES: Enter any limitations on further dissemination of the report, other than those imposed by security classification, using standard statements such as:

(1) "Qualified requesters may obtain copies of this report from DDC."

(2) "Foreign announcement and dissemination of this report by DDC is not authorized."

(3) "U. S. Government agencies may obtain copies of this report directly from DDC. Other qualified DDC users shall request through _____."

(4) "U. S. military agencies may obtain copies of this report directly from DDC. Other qualified users shall request through _____."

(5) "All distribution of this report is controlled. Qualified DDC users shall request through _____."

If the report has been furnished to the Office of Technical Services, Department of Commerce, for sale to the public, indicate this fact and enter the price, if known.

11. SUPPLEMENTARY NOTES: Use for additional explanatory notes.

12. SPONSORING MILITARY ACTIVITY: Enter the name of the departmental project office or laboratory sponsoring *(paying for)* the research and development. Include address.

13. ABSTRACT: Enter an abstract giving a brief and factual summary of the document indicative of the report, even though it may also appear elsewhere in the body of the technical report. If additional space is required, a continuation sheet shall be attached.

It is highly desirable that the abstract of classified reports be unclassified. Each paragraph of the abstract shall end with an indication of the military security classification of the information in the paragraph, represented as *(TS)*, *(S)*, *(C)*, or *(U)*.

There is no limitation on the length of the abstract. However, the suggested length is from 150 to 225 words.

14. KEY WORDS: Key words are technically meaningful terms or short phrases that characterize a report and may be used as index entries for cataloging the report. Key words must be selected so that no security classification is required. Identifiers, such as equipment model designation, trade name, military project code name, geographic location, may be used as key words but will be followed by an indication of technical context. The assignment of links, roles, and weights is optional.